Crossed Beam Collision Mechanics: Reactions of Ca, Sr, and Ba with HI and Limits on D_0° for CaI, SrI, and BaI

Cite as: J. Chem. Phys. **57**, 3099 (1972); https://doi.org/10.1063/1.1678726
Submitted: 20 March 1972 . Published Online: 03 September 2003

Charles A. Mims, Shen-Maw Lin, and Ronald R. Herm

Crossed Beam Collision Mechanics: Reactions of Ca, Sr, and Ba with HI and Limits on $D_0°$ for CaI, SrI, and BaI

CHARLES A. MIMS, SHEN-MAW LIN, AND RONALD R. HERM*

Inorganic Materials Research Division, Lawrence Berkeley Laboratory and Department of Chemistry, University of California, Berkeley, California 94720

(Received 20 March 1972)

Angular distributions of MI (M=Ca, Sr, or Ba) products scattered from crossed beams of HI and M are reported and compared with derived expressions for the angular distributions of the velocities of the center-of-mass. These comparisons indicate that the reaction threshold relative kinetic energies, E^*, are 5, 4, and 2.5 kcal/mole for the Ca, Sr, and Ba+HI reactions, respectively. Energy conservation and these measured E^* values establish rigorous lower bounds for $D_0°$(MI) of 64 (CaI), 65(SrI), and 66 (BaI) kcal/mole.

The K+HBr→KBr+H reaction was the first studied by the crossed molecular beam technique.[1] Reactions of A+HB→AB+H where the masses of both A and B greatly exceed that of the hydrogen atom are kinematically unique in that the nature of the transformation between the laboratory (LAB) and center-of-mass (CM) coordinate systems requires[2] that the AB product appear in the LAB system with a velocity close to that of the velocity of the center-of-mass of the collision partners, **C**. This makes it extremely difficult to elucidate the reaction energy and angle recoil distributions from measurements of the AB flux in the LAB, although Bernstein and co-workers[3] did manage to do so for the K+HBr and K+DBr reactions in an elegant experiment employing a velocity selected K beam and velocity analysis of the KBr product. However, this kinematic restriction on these reactions makes possible the determination of the dependence of the reaction cross section, Q, on relative kinetic collision energy, E, by means of an experiment in which the two reactant beams are crossed with known velocity distributions. Here one argues that the heavy AB product which is detected must essentially recoil (in the LAB) along **C** and exploits the broad distribution in E by proceeding to calculate the angular distributions of **C** for various assumed forms of $Q(E)$. The requisite theory was developed in Ref. 2 for a crossed thermal beams experiment in which the LAB flux of AB product is measured and was applied to the data reported in Ref. 1 for the K+HBr reaction. This resulted in an estimated threshold relative kinetic energy, E^*, of ~2.5–3 kcal/mole, although the agreement of the experimental data with the theoretical curve was not very good. A much smaller value of E^* for this K+HBr reaction was obtained in a more recent[4] measurement of the KBr flux formed upon crossing a velocity selected K beam by a thermal HBr beam. A recent crossed thermal beams experiment of the type analyzed in Ref. 2 has reported[5] E^*~2–3 kcal/mole for the K+HCl→KCl+H reaction.

Although gaseous reactions of group IIa alkaline earth atoms have apparently not yet been studied by conventional kinetics techniques, a number of molecular beam laboratories,[6–11] including our own, have recently become interested in reactions of these atoms. In the work reported here, analyses of measured product MI (M=Ca, Sr, or Ba) LAB angular distributions provide values of E^* for the M+HI→MI+H reactions as well as rigorous lower limits on $D_0°$ (MI).

EXPERIMENTAL PROCEDURE

The apparatus is described in detail in Ref. 12. Although less versatile and sensitive, it is similar to the universal detector molecular beam scattering apparatus described in Ref. 13. The alkaline earth atom beam emerges from a knife-edge slit (0.05 cm wide×0.5 cm high) in a resistively heated, single-chamber stainless steel oven; source pressures of ~0.25, ~0.35, and ~0.3 torr for the Ba, Sr, and Ca experiments, respectively, are employed. The HI, at a reservoir pressure of ~2 torr, emerges from a "crinkly foil" many-channel source [a slit, 0.16 cm wide×~0.7 cm high, prepared by alternately stacking layers of flat and 0.01 cm wide corrugated stainless steel foil (0.0025 cm foil thickness)] at a gas flow rate of ~70 cm³/sec, resulting in an ambient apparatus background pressure of ~4×10^{-6} torr. The HI beam is chopped at ~39 Hz and intersects the atom beam at 90°, resulting in a weak (~1%–5%) attenuation of the atom beam. Figure 1 shows the profiles of the two beams. An H_2 impurity in the HI beam is of no consequence, but an I_2 impurity is troublesome because it produces significant (relative to the HI contribution) alkaline earth iodide scattered signal. Contributions from scattering from I_2 were shown to be negligible (1) by the absence of an I_2 signal in the mass spectrum of the main beam and (2) by checking that no alkaline earth iodide was scattered into negative LAB angles.

The detector, housed in a differentially pumped UHV chamber and able to see the entire beam collision zone, may be rotated in the plane defined by the two intersecting beams. The scattered species are ionized by electron bombardment, mass analyzed in an RF quadrupole massfilter, and detected, via electron multiplier amplification, by means of a PAR HR-8

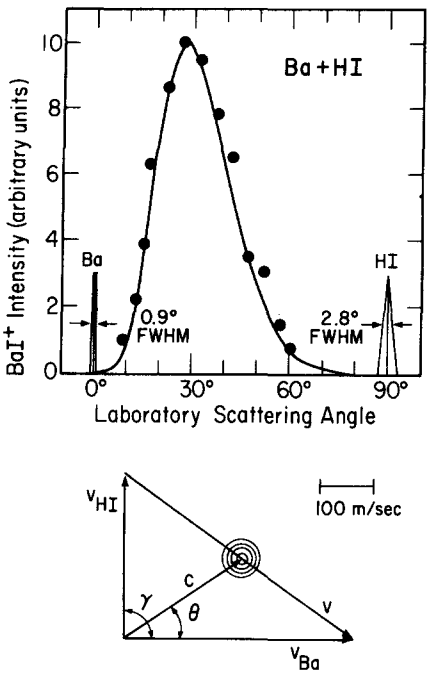

FIG. 1. The data points show measured LAB angular distributions of BaI product of the Ba+HI reaction; nominal beam temperatures: 1033°K (Ba) and 363°K (HI). The solid curve gives the number density angular distribution of C, $B(\theta)$, calculated from Eq. (7) for reaction model B [Eq. (13b)] for $E^*=2.5$ kcal/mole by numerical integration over the experimentally measured speed distributions in the two beams. Also shown are angle profiles of the two beams as well as a LAB↔CM transformation diagram for the Ba+HI reaction. This is drawn for the $\gamma=90°$ intersection angle employed in this work and for the Ba and HI most probable beam speeds and shows the relative collision velocity, V, and velocity of the center-of-mass, C. The circles are drawn for BaI CM recoil speeds corresponding to typical possible product recoil energies of 1, 3, 6, and 10 kcal/mole.

lock-in amplifier referenced (with negligible phase shift) to the HI beam chopping frequency.

CROSSED BEAM COLLISION MECHANICS

Expressions for the number density angular distributions of C which are derived in this section are obtained by an extension of the methods and results given in Ref. 2; accordingly, the nomenclature employed in Ref. 2 is retained here. Two beams of particle masses M_1 and M_2 are assumed to collide at an angle γ defining an intersection volume τ. The relative collision velocity, V, relative collision energy, E, and center-of-mass velocity, C, are defined in terms of the velocities of particles in beams 1 and 2, $\mathbf{v}_1$ and $\mathbf{v}_2$, by:

$$\mathbf{V}=\mathbf{v}_1-\mathbf{v}_2, \tag{1a}$$

$$M\mathbf{C}=M_1\mathbf{v}_1+M_2\mathbf{v}_2, \tag{1b}$$

and

$$E=\mu V^2/2, \tag{1c}$$

where the mass factors are given by

$$M=M_1+M_2 \tag{2a}$$

and

$$\mu=M_1M_2/M. \tag{2b}$$

Figure 1 includes a transformation diagram illustrating the relations of $\mathbf{v}_1$, $\mathbf{v}_2$, V, C, and θ, the angle between $\mathbf{v}_1$ and C.

The number of reactive events per second, N, may be written in terms of the number densities of beams 1 and 2 at the collision zone, n_1 and n_2, as

$$N=n_1n_2r\int_0^\infty\int_0^\infty Q(V)V\rho_1(v_1)\rho_2(v_2)dv_1dv_2, \tag{3}$$

where ρ_1 and ρ_2 are the number density probability density speed distribution functions for beams 1 and 2. This may also be written as

$$N=\int_0^\gamma\int_0^\infty P(\theta, C)dCd\theta, \tag{4}$$

where $P(\theta, C)dCd\theta$ is the number of reactive collisions per second with center-of-mass speed between C and $C+dC$ and direction between θ and $\theta+d\theta$. Equating N in Eqs. (3) and (4), $P(\theta, C)$ may be written as

$$P(\theta, C)=n_1n_2rQ(V)V\rho_1(v_1)\rho_2(v_2)M^2C/M_1M_2\sin\gamma; \tag{5}$$

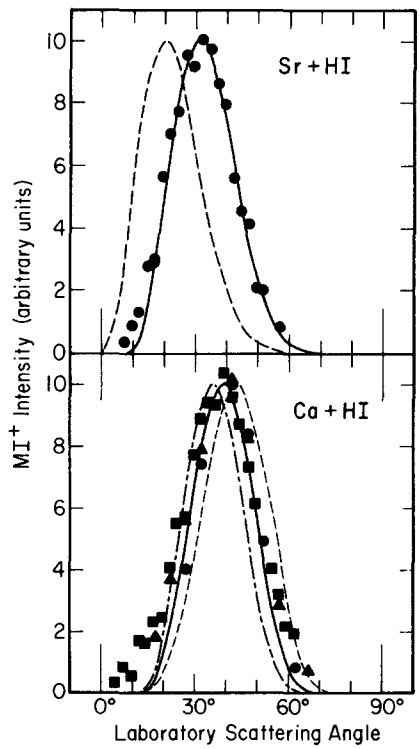

FIG. 2. Data points give measured product LAB angular distributions of SrI and CaI; different data point symbols for CaI show results measured on different pumpdowns; nominal beam temperatures: 953 and 348°K for Sr+HI; 1020 and 328°K for Ca+HI. Also shown are $B(\theta)$ curves calculated as described for Fig. 1 for: Sr+HI for $E^*=4$ kcal/mole (solid); and Ca+HI for $E^*=3$ (dash), 5 (solid), and 7 (dash-dot) kcal/mole. The $B(\theta)$ function calculated for $E^*=4$ kcal/mole and reaction model B for intersecting Sr and HI beams with thermal speed distributions is also shown (dash curve).

V, v_1, and v_2 may be expressed as functions of θ and C by means of the transformation equations given in Ref. 2. Integration of $P(\theta, C)$ over C yields the flux angular distribution of **C**. However, the electron bombardment ionizer is a number density detector so that the appropriate centroid distribution function becomes

$$B(\theta, C)=\delta P(\theta, C)/C, \tag{6}$$

where δ is a constant characterizing the detector sensitivity. The angular distribution of **C** appropriate to experiments employing a number density detector is then given by

$$B(\theta)=\int_0^\infty B(\theta, C)dC. \tag{7}$$

Crossed Thermal Beams

The expressions for $B(\theta, C)$ and $B(\theta)$ are especially simple in the case of two crossed beams with thermal speeds distributions. For this thermal case, $B(\theta, C)$ becomes

$$B(\theta, C)=\beta Q(MC/m)F(\theta)C^5\exp[-M^2C^2/m^2\alpha^2],$$
$$F(\theta)=m^{-1}\sin^2(\gamma-\theta)\sin^2\theta/\sin^5\gamma, \tag{8}$$

where $MC/m=V$, $\beta=16\delta n_1n_2\tau M^7/\pi M_1^3M_2^3\alpha_1^3\alpha_2^3$, and α_1 and α_2 are the most probable thermal source speeds, $\alpha_i=(2kT_i/M_i)^{1/2}$. Equation (8) is written in terms of the velocity independent, angle dependent "effective mass" m and "effective thermal source speed" α derived in Ref. 2 as

$$m^{-2}\sin^2\gamma=\frac{\sin^2(\gamma-\theta)}{M_1^2}-\frac{2\cos\gamma\sin(\gamma-\theta)\sin\theta}{M_1M_2}+\frac{\sin^2\theta}{M_2^2}, \tag{9}$$

$$\alpha^2=\frac{\sin^2\gamma}{m^2}\left(\frac{\sin^2(\gamma-\theta)}{M_1^2\alpha_1^2}+\frac{\sin^2\theta}{M_2^2\alpha_2^2}\right)^{-1}. \tag{10}$$

Molecular beam experimentalist may occasionally want to employ Eq. (8) directly. Thus, assuming that $Q(E)$ were known, comparison of Eq. (8) with measured LAB velocities of the AB product of the kinematically constrained A+HB reaction would provide a check against systemtic apparatus errors. Additionally, this equation indicates the distribution in origin of the CM coordinate system and might be useful in estimating the loss of resolution in CM cross sections which results from the LAB→CM transformation for the case of crossed thermal beam experiments.

In analogy with observations in Ref. 2, $B(\theta)$ obtained by substitution of the $B(\theta, C)$ expression of Eq. (8) into Eq. (7) is naturally expressed as

$$B(\theta)=(\beta/2)(m/M)^6F(\theta)G(\alpha^{-2}) \tag{11}$$

in terms of the Laplace transform

$$G(\alpha^{-2})=\int_0^\infty \exp(-Z/\alpha^2)Z^2Q(Z)dZ, \tag{12}$$

where $Z=2E/\mu$. This transform is known[14] for the following two simple forms of $Q(E)$:

$$Q_A(E)=Q_0u(E-E^*), \tag{13a}$$
$$Q_B(E)=Q_0[1-(E^*/E)]u(E-E^*). \tag{13b}$$

Here, Q_0 and E^* are constants and $u(t)$ is the unit step function, i.e.,

$$u(t)=0 \quad \text{for} \quad t<0,$$
$$u(t)=1 \quad \text{for} \quad t>0.$$

Model B is the well known form of $Q(E)$ which assumes a step function dependence on the component of collision energy directed along the line-of-centers at impact. The $B(\theta)$ functions obtained from Eq. (11) for the cross section models given in Eqs. (13a) and (13b) become:

$$B_A(\theta)=B_0(\theta)[2\alpha^6+2V^{*2}\alpha^4+V^{*4}\alpha^2] \tag{14a}$$

and

$$B_B(\theta)=B_0(\theta)[2\alpha^6+V^{*2}\alpha^4], \tag{14b}$$

where $E^*=\mu V^{*2}/2$ and $B_0(\theta)$ is given by

$$B_0(\theta)=(\beta Q_0/2)(m/M)^6F(\theta)\exp(-V^{*2}/\alpha^2). \tag{15}$$

Note that $B_A(\theta)$ and $B_B(\theta)$ are identical in the limit that $E^*=0$. A detailed discussion of the dependences of $B_A(\theta)$ and $B_B(\theta)$ on V^* and γ is given in Ref. 12(a). Here again, these expressions should be useful to molecular beam experimentalist, as a comparison of a measured LAB product angular distribution with $B(\theta)$ allows one to quickly estimate the tendency of the reaction to scatter the product into the forward versus the backward hemisphere in the CM coordinate system.

EXPERIMENTAL RESULTS

The LAB↔CM transformation diagram for the Ba+HI reaction which is included in Fig. 1 indicates that the LAB BaI scattering velocity could deviate significantly in direction from that of **C**. The maximum possible deviation may be estimated from the largest BaI CM recoil speed shown in the diagram, as the reaction is unlikely to be exothermic by more than the ~10 kcal/mole exothermicity of the analogous Cs+HI reaction. The extent of possible deviations for the Sr and Ca reactions should resemble that for the Ba reaction because the decreasing M_{MI}/M_H mass ratio is offset by the likely decrease in the reaction exothermicities. However, two arguments suggest that the deviations between the directions of **C** and the LAB MI velocities should be insignificant: (1) The product KBr velocity analysis experiments reported in Ref. 3(b) indicate that a large fraction of the reactions of K with HBr and DBr produce low product recoil energies, E'; and (2) the peak in the LAB MI angular distribution is most sensitive to reactions producing low E' values because of the form of the Jacobian of the CM→LAB transformation. As an additional argu-

TABLE I. M+HI→H+MI reaction threshold energies and lower limits for $D_0°$ (MI).[a]

Group IIa atom, M	Measured threshold relative collision energy, E^*	$D_0°$ (MI) estimates of Ref. 18	Lower limits for $D_0°$ (MI) provided by this work
Ca	5±1	75±15	64
Sr	4±1	80±15	65
Ba	2.5±1	85±15	66

[a] All energies are given in kcal/mole.

ment against a significant deviation from **C**, MI LAB angular distributions for the Ca, Sr, and Ba+HI reactions were calculated for various assumed CM angular and E' distributions by numerical integrations of the CM→LAB transformation. The calculated MI LAB angular distributions were always broader than the calculated angular distributions of **C**, although the additional breadths were negligible unless the E' values were predominately confined to values greater than ~5 kcal/mole.

The Beam Speed Distributions

The measured LAB BaI, SrI, and CaI product angular distributions are shown in Figs. 1 and 2. It proved impossible to fit these measured LAB distributions to angular distributions of **C** calculated for thermal beams by means of Eqs. (14a) or (14b). In view of the relatively good angular resolution employed here, this failure suggested a nonthermal speed distribution for at least one of the beams, and a small, slotted cylinder velocity selector described in Ref. 12(a) was employed to measure the actual beam speed distributions.

Other workers[15] have reported a nonthermal speed distribution for a beam source similar to the multichannel HI source employed here. Empirically, our velocity selector measurements are well fit by an HI number density speed probability distribution of the form

$$\rho_2(v_2) = (v_2-u_2)^2 \exp[-(v_2-u_2)^2/\alpha_2^2]u(v_2-u_2), \quad (16)$$

where α_2 is still the HI most probable thermal source speed and $u(t)$ is the unit step function. The "flow speed," u_2, increases with increasing HI source pressure; for the 2 torr source pressure employed here the speed distribution is considerably nonthermal with $u_2=0.45\alpha_2$.

The alkaline earth beam source conditions are close to the conditions for thermal effusion. Space and signal-to-noise limitations prevented a measurement of the Sr and Ca beam speed distributions. However, even for 1 torr source pressure, the measured Ba beam speed distribution shows much less deviation from thermal behavior than the HI distribution. The deviations from thermal behavior which are observed correspond to an attenuation of the low speed portion of the thermal distribution. The magnitudes of these attenuations are similar to those reported in the early molecular beam literature[16] and attributed to beam–beam scattering.

Reaction Threshold Energies

Angular distributions of **C** were calculated from Eq. (7) by numerical integration over the measured beam speed distributions. The solid curves in Figs. 1 and 2 show the $B(\theta)$ functions calculated from E^* values which best fit the data, using reaction model B [Eq. (13b)]. In performing the calculations, the Sr and Ca beam speed distributions were estimated by applying the thermal attenuation factor for a given v_1/α_1 which was derived from the measured Ba speed distribution. The approximate theory of the beam–beam scattering developed in Ref. 16 indicates that this procedure should be correct for constant collision cross sections. Since the Sr–Sr and Ca–Ca collision cross sections should be less than that of Ba–Ba, this procedure may overestimate the deviations of these beams from thermal behavior. In practice, this small uncertainty in the Sr and Ca speed distributions is inconsequential because calculations of $B(\theta)$ for thermal atom beam speed distributions are practically indistinguishable from the $B(\theta)$ curves shown in Figs. 1 and 2.

In general, the fits of the theoretical $B(\theta)$ curves to the measured MI signals which are shown in Figs. 1 and 2 are very good, much better than was obtained in previous studies of the K+HBr[2] and HCl[5] reactions. The small positive deviations of the measured MI signals from the calculated $B(\theta)$ curves which are apparent at small LAB angles in Figs. 1 and 2 are probably a consequence of Eq. (16), which unrealistically assumes zero probability for very small HI speeds and thereby renders the calculated $B(\theta)$ curves absolutely zero at small θ values.

The Sr+HI panel in Fig. 2 also shows a $B(\theta)$ curve calculated for two thermal beam speed distributions and reflects the sensitivity of the $B(\theta)$ calculations to the true HI beam speed distribution. The Ca+HI panel in Fig. 2 includes calculations of $B(\theta)$ curves for three different values of E^* in order to indicate the sensitivity of the fit to the data to the E^* value; the Ca+HI data is the least sensitive to changing E^* values because this reaction has the highest threshold energy. In general, reaction cross section model A [Eq. (13a)] provides $B(\theta)$ curves which fit the data as well as the model B calculations illustrated in the figures; model A provides best fits for E^* values slightly larger (~0.5 kcal/mole) than those obtained from model B fits. Table I lists the E^* values which best fit the data shown in Figs. 1 and 2; the uncertainties in E^* listed in the table reflect the differences between models A and B fits as well as the range in E^*

values which adequately fit the data for calculations for one reaction model.

Other Reactions

No reactively scattered MX signals were observed from crossed beams of either Mg and HI or Ba and HF. If one assumes that the Q_0 constants in Eq. (13) for these reactions are comparable to those for Ca, Sr, and Ba+HI, this inability to observe reaction in the apparatus employed here would imply that $E^*>\sim 8$ kcal/mole for these two reactions. This might simply be a consequence of the Mg+HI reaction energetics, as $D_0°(\mathrm{MgI})$ is not known well, but is likely[17,18] to be considerably less than $D_0°(\mathrm{HI})$. However, the behavior of the Ba+HF reaction cannot be rationalized in this manner, as the most recent value[19] for $D_0°(\mathrm{BaF})$ exceeds that of $D_0°(\mathrm{HF})$ by ~ 5 kcal/mole.

CaI, SrI, AND BaI BOND DISSOCIATION ENERGIES

As the techniques are applied to a wider variety of chemical reactions, studies of reaction dynamics may be expected to establish limits on a number of bond dissociation energies which are difficult to measure directly. For example, recent molecular beam electronic chemiluminescence experiments[6] have established lower limits on $D_0°$ of BaO, BaCl, and SrCl. In the experiments reported here, a minimum of E^* relative kinetic energy is shown to be sufficient for the reactions of Ca, Sr, and Ba with HI. At the temperatures employed, the HI has negligible vibrational excitation and an average rotational energy given[20] by RT_{HI}. The product recoil energy, E', and internal excitation, W', are related by energy conservation to the reactant energy by

$$D_0°(\mathrm{MI})=D_0°(\mathrm{HI})-E^*-RT_{\mathrm{HI}}+E'+W'. \quad (17)$$

In his most recent compilation of bond energies of diatomic molecules, Gaydon[17] regards the experimental data on the bond energies of CaI, SrI, and BaI as unreliable and refers to ionic model calculations by Krasnov and Karaseva[18] for the best estimates. Since $D_0°(\mathrm{HI})$ is known[17] to be 70.6 kcal/mole, rigorous lower limits on $D_0°$ of CaI, SrI, and BaI may be calculated from Eq. (17) and upper limits for E^* given in Table I by assuming the $E'+W'=0$. Table I shows a comparison of these lower limits with the ionic model estimates reported in Ref. 18.

ACKNOWLEDGMENTS

This work was supported by the U.S. Atomic Energy Commission through the Lawrence Berkeley Laboratory. Partial support from the Committee on Research of the University of California at Berkeley is also gratefully acknowledged.

* Alfred P. Sloan Foundation Fellow.
[1] E. H. Taylor and S. Datz, J. Chem. Phys. **23,** 1711 (1955).
[2] S. Datz, D. R. Herschbach, and E. H. Taylor, J. Chem. Phys. **35,** 1549 (1961).
[3] (a) A. E. Grosser, A. R. Blythe, and R. B. Bernstein, J. Chem. Phys. **42,** 1268 (1965); (b) K. T. Gillen, C. Riley, and R. B. Bernstein, *ibid.* **50,** 4019 (1969).
[4] D. Beck, E. F. Greene, and J. Ross, J. Chem. Phys. **37,** 2895 (1962).
[5] T. J. Odiorne and P. R. Brooks, J. Chem. Phys. **51,** 4676 (1969).
[6] (a) Ch. Ottinger and R. N. Zare, Chem. Phys. Letters **5,** 243 (1970); (b) C. D. Jonah and R. N. Zare, *ibid.* **9,** 65 (1971); (c) C. D. Jonah, R. N. Zare, and Ch. Ottinger, J. Chem. Phys. **56,** 263 (1972).
[7] C. Batalli-Cosmovici and K. W. Michel, Chem. Phys. Letters **11,** 245 (1971).
[8] J. Fricke, B. Kim, and W. L. Fite, *Abstracts of Papers of the 7th International Conference on the Physics of Electronic and Atomic Collisions* (North-Holland, Amsterdam, 1971), pp. 37–38.
[9] F. Engelke, Universität Freiburg (private communication).
[10] J. A. Haberman, K. G. Anlauf, R. B. Bernstein, and F. J. Van Itallie, Chem. Phys. Letters, "Primitive Product Angular Distributions for the Crossed Beam Reactions of Ba with NO_2 and Cl_2" (to be published).
[11] D. R. Herschbach, Harvard University (private communication).
[12] (a) C. A. Mims, Ph.D. thesis, University of California, Berkeley, California, 1972; (b) S.-M. Lin, Ph.D. thesis, University of California, Berkeley, California, 1972.
[13] Y. T. Lee, J. D. McDonald, P. R. LeBreton, and D. R. Herschbach, Rev. Sci. Instr. **40,** 1402 (1969).
[14] M. Abramowitz and I. A. Stegun, Natl. Bur. Std. (U.S.) Appl. Math. Ser. **55,** 1020–1030 (1964).
[15] N. C. Blais and J. B. Cross, J. Chem. Phys. **52,** 3580 (1970).
[16] I. Estermann, O. C. Simpson, and O. Stern, Phys. Rev. **71,** 238 (1947).
[17] A. G. Gaydon, *Dissociation Energies and Spectra of Diatomic Molecules* (Chapman and Hall, London, 1968), 3rd ed.
[18] K. S. Krasnov and N. V. Karaseva, Opt. Spectrosc. **19,** 14 (1965).
[19] D. L. Hildebrand, J. Chem. Phys. **48,** 3657 (1968).
[20] Actually, the HI rotational energy might be less than RT_{HI} if the enhanced HI speed distribution reflected a transition to an isentropic nozzle flow. However, this is a minor effect which would make the lower limits on $D_0°(\mathrm{MI})$ given in Table I be too low by less than 0.5 kcal/mole.